

Supporting Information to the paper

A Two-Step Spin-Crossover Mononuclear Iron(II) complex with a [HS-LS-LS] Intermediate Phase

Sylvestre Bonnet,^a Maxime A. Siegler,^b José Sánchez Costa,^a Gábor Molnár,^c
Azzedine Bousseksou,^c Anthony L. Spek,^b Patrick Gamez,^a
and Jan Reedijk^{*,a}

^a *Leiden Institute of Chemistry, Leiden University, P.O. Box 9502, 2300 RA
Leiden, The Netherlands;*

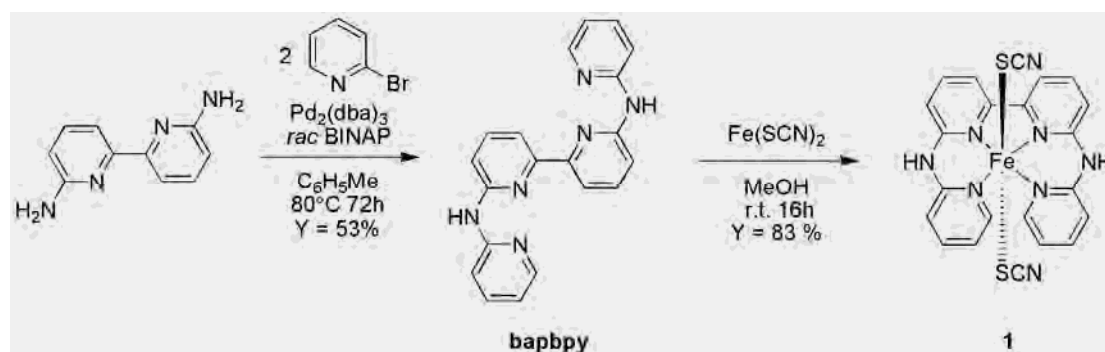
^b *Bijvoet Center for Biomolecular Research Crystal and Structural Chemistry,
Utrecht University, Padualaan 8, 3584 CH Utrecht, The Netherlands;*

^c *Laboratoire de Chimie de Coordination, UPR 8241 CNRS, 205 Route de
Narbonne, 31077 Toulouse, France*

Table of contents

Preparation of the ligand bapbpy and details for the preparation of complex 1	2–3
Magnetic measurements and single crystal X-ray structure determinations	4–6
Figure S1. Crystal packing of the HS phase of complex 1 (phase I).	6
Figure S2. Representations of the single crystal X-ray structures of phases II and III of 1 .	7
Figure S3. Crystal packing of the IP and LS phase of complex 1 (phases II and III)	7
Table S1. Selected bond lengths and angles for the three phases of 1	8
Table S2. Hydrogen bonding interactions in the three phases of 1	9
Table S3. π – π bonding interactions in the three phases of 1	9
Figure S4. Crystal packings of the three phases down the <i>b</i> direction	10
Figure S5. Crystal packing of the intermediate phase II of complex 1 showing the remarkable [HS...LS...LS] motif	10
Figure S6. X-ray diffraction patterns for the phases I , II and III	11
Figure S7. Plots of the cell dimensions <i>a</i> (Å), <i>b</i> (Å), <i>c</i> (Å) and β (°) for 1 determined from 260 to 160 K at –4 K intervals and from 160 to 260 K at 4 K intervals.	12
Figure S8. DSC analysis for 1	13

Preparation of **babppy** and its complex $[\text{Fe}(\text{babppy})(\text{NCS})_2]$ (**1**)



6,6'-Diamino-2,2'-bipyridine was synthesized from 6,6'-dibromo-2,2'-bipyridine¹ according to a literature procedure.²

babppy: 562 mg of 6,6'-diamino-2,2'-bipyridine (3.02 mmol), 55 mg of $\text{Pd}_2(\text{dba})_3$ (0.060 mmol, 2 mol% in Pd per C–Br bond), 75 mg of racemic BINAP (0.12 mmol, 2 mol% per C–Br bond), and 1.36 g of KO^tBu (12.1 mmol, 4 eq.) were weighed in a dry schlenk and put under argon. 30 mL of dry, degassed toluene and 0.88 mL of 2-bromopyridine (9.0 mmol, 3.0 eq.) were added, and the mixture was heated to 80°C and stirred under argon for 3 days. The resulting orange suspension was cooled to room temperature and 150 mL of water were added. The mixture was stirred vigorously for 1 h, upon which the orange color disappeared. The solid was filtered and washed with water, diethylether, and dried under vacuum. Yield: 837 mg as a slightly brown solid (81%).

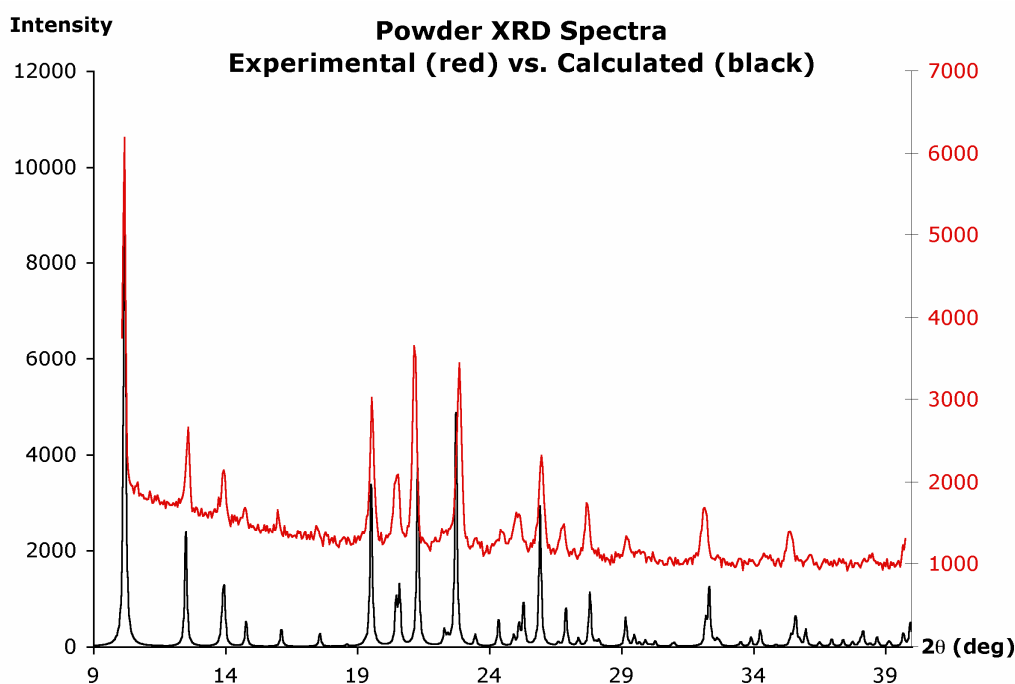
Purification: 10 g of neutral alumina and 50 mL of dichloromethane were added to the crude compound. The solvent was evaporated in a rotary evaporator, and the resulting solid was put on top of a column chromatography (150 mL; neutral alumina). Elution with dichloromethane containing 0.2 to 10% methanol afforded 565 mg of pure **babppy** as a light yellow powder (55%).

^1H NMR (300 MHz, δ_{ppm} in $\text{DMSO}-d_6$): 9.80 (s, 2H, NH), 8.25 (d, 2H, J 3.8 Hz), 7.96 (d, 2H, J 8.4 Hz), 7.85 (m, 4H), 7.73 (t, 2H, J 8.5 Hz), 7.69 (t, 2H, J 7.4 Hz), 6.91 (t, 2H, J 5.2 Hz). ^{13}C NMR (75 MHz, δ_{ppm} in $\text{DMSO}-d_6$): 154.3, 153.9, 153.5, 147.5, 138.4, 137.6, 116.0, 112.4, 112.1, 111.6. ES MS m/z (calc): 340.8 (340.4, $[\text{M}]^+$). IR (cm^{-1}): 3230.2, 3168.0, 3080.7, 3043.8, 3015.2, 2931.7, 1608.1, 1593.7, 1575.6, 1557.6, 1532.0, 1526.0, 1481.9, 1417.8 (strong), 1343.9, 1298.5, 1270.3, 1233.2, 1148.4, 1073.4, 993.6, 984.0, 793.0, 765.2, 732.5, 667.9, 629.6, 598.1, 569.4, 515.5, 429.8, 404.4, 361.1, 327.8, 324.1. LF spectroscopy (solid state): $\lambda_{\text{max}} = 279, 348, 370$ nm. The elemental analysis was performed on a sample of **babppy** obtained after recrystallization from hot DMF, under argon. Anal. Calcd. for $\{\text{C}_{20}\text{H}_{16}\text{N}_6 + (\text{DMF})_{0.5}\}$: C, 68.51; H, 5.21; N, 24.15. Found: C, 68.92; H, 4.98; N, 24.08.

The 0.1 M methanolic solutions of $[\text{Fe}(\text{SCN})_2]$ used for the synthesis of complex **1** were prepared as follows: 277 mg (1.00 mmol) of $\text{FeSO}_4 \cdot 7\text{H}_2\text{O}$ and 194 mg (2.00 mmol) of KSCN were mixed in 6 mL of methanol and stirred for 30 min. 5 mg of ascorbic acid were added to afford a

colorless suspension (ascorbic acid prevents the oxidation of Fe(II) to Fe(III)). K_2SO_4 was filtered off over a 10 mL volumetric flask. The flask was filled to 10.0 mL with methanol resulting in a clear, colorless iron(II) solution which must be used immediately. See article for the synthesis of complex **1**.

Note: The X-ray powder diffraction spectrum at room temperature of a crude powder sample of complex **1** obtained at the end of the synthesis corresponds to the theoretical spectrum calculated from the single crystal X-ray structure at 295 K of the recrystallized complex (phase **I**, see Figure below). Reversely, the IR spectrum of crushed monocrystals of complex **1** is identical to that of the crude powder. Both tests favour similar compositions for the crude and recrystallized compounds.



References

- ¹ Bai, X.-L.; Liu, X.-D.; Wang, M.; Kang, C.-Q.; Gao, L.-X. *Synthesis* **2005**, *3*, 458-464.
- ² Thibault, M. E., Luska, K. L., Schlaf, M. *Synthesis* **2007**, *5*, 791-793.

Magnetic measurements

The measurement of $\chi_m T = f(T)$ was performed on a sample made of 4.87 mg of monocrystals of **1** obtained by recrystallization of the crude compound from DMF / MeOH, as indicated in the Experimental Part. The sample is hence a loosely packed collection of randomly oriented single crystals. The sample was mounted on a plastic straw before introduction in a Quantum Design MPMS-XL squid magnetometer. DC magnetization measurements were performed in a field of 0.5 T, from 300 to 3 K (cooling mode) and from 3 to 300 K (heating mode). The total measuring time was 20 h. Corrections for the diamagnetism of the sample were calculated using Pascal's constants.

Single-crystal X-ray diffraction studies

All reflection intensities were measured using a Nonius KappaCCD diffractometer (rotating anode) with graphite-monochromated Mo $K\alpha$ radiation ($\lambda = 0.71073 \text{ \AA}$) under the program *COLLECT*.¹ The program *PEAKREF*² was used to determine the cell dimensions. All sets of data were integrated using the program *EVALCCD*³. All structures were solved with the program *DIRDIF99*⁴ or with *SHELXS86*⁵ and were refined on F^2 with *SHELXL97*.⁶ Multi-scan semi-empirical absorption corrections were applied to all sets of data with the program *SADABS*⁷ or with *TWINABS*.⁸ The temperature of the data collection was controlled using the system *OXFORD CRYOSTREAM 600* (manufactured by *OXFORD CRYOSYSTEMS*). The H-atoms (except for those attached to the N atoms) were placed at calculated positions (*AFIX 43*) with isotropic displacement parameters having values 1.2 times U_{eq} of the attached C atom. The H-atoms attached to the N atoms were found in the difference Fourier map and the N–H bond distances were restrained to be 0.86 Å (at 295 K) or 0.88 Å (at 110 and 190 K) using the *DFIX* instruction. The atom-numbering scheme was made consistent for the three phases (Figures 1 and S2).

For all sets of measurements (i.e., the data collection for phases **I**, **II**, and **III** and the data for the temperature dependences of the cell dimensions), the same crystal was used since no significant loss of crystallinity occurs as the crystal was either cooled or heated.

Data for the ordered phase **I** ($C2/c$, $Z' = 1/2$) were collected at 295(2) K. The Fe complex is located at sites of twofold symmetry.

The structure of the ordered phase **II** was originally solved in the centro-symmetric space group $C2/c$ with $Z' = 1 + 1/2$ (because the Fe LS of the complex is located at sites of twofold symmetry). Data for this phase were collected at 190(1) K after the crystal had been slowly cooled at -2 K/min from room temperature. The cell constants of the conventional C -centred cell at 190 K are: $a = 15.7348(2) \text{ \AA}$, $b = 10.7200(3) \text{ \AA}$, $c = 38.0533(6) \text{ \AA}$, $\beta = 94.859(1)^\circ$. The non-conventional C -centred cell was preferred so that the cell of phase I and that of phase II can be easily compared.

The transformation matrix \mathbf{M} that converts the conventional cell into the non-conventional cell is given by $\mathbf{M} = (1\ 0\ 0 / 0\ 1\ 0 / -1\ 0\ 1)$. An additional origin shift of $(a + b)/4$ was applied so that the space group remains unchanged after transformation (the space group would be $C2/n$ if no origin shift was applied).

The structure of the ordered phase **III** was originally solved in the centro-symmetric space group $P\bar{1}$ with $Z' = 1$. Data for this phase were collected at 110(1) K after the crystal had been slowly cooled at -2 K/min from room temperature. The cell constants of the primitive cell at 110 K are: $a = 9.4494(6)$ Å, $b = 9.5068(4)$ Å, $c = 13.4735(6)$ Å, $\alpha = 94.437(2)^\circ$, $\beta = 105.989(2)^\circ$, $\gamma = 112.198(3)^\circ$. The non-standard space group $C\bar{1}$ was preferred so that the cells of phases I and III are similar. The transformation matrix \mathbf{M} that converts the primitive cell into the non-standard C -centred cell is given by $\mathbf{M} = (-1\ 1\ 0 / -1\ -1\ 0 / 1\ 0\ 1)$. The structure of this phase is non-merohedrally twinned. In the process of determining the cell dimensions, the program *DIRAX*⁹ found the twin relationship for which the two domains are related by a twofold axis along the $[1\ 1\ 0]$ direction in the primitive cell (*i.e.*, the b direction in the C -centred cell). The fractional contribution of the minor twinned component refined to 0.476 (1).

Temperature dependences of the cell dimensions

One set of data using an automatic procedure based on the phi/chi cell determination method¹⁰ was measured in order to derive the temperature dependences of the cell dimensions in both cooling and heating regimens. No significant loss of crystallinity occurs as the crystal was either cooled or heated. All reflection intensities (*i.e.*, near 300 reflections for phase **I**, near 470 reflections for phase **II** and near 360 reflections for phase **III**) were measured between 260 and 160 K at -4 K intervals (cooling) and between 160 and 260 K at 4 K intervals (heating) using a Nonius KappaCCD diffractometer equipped with a fine-focus sealed tube. The crystal to detector distance was fixed at 60 mm throughout the whole series of measurements. The localization of the two cooling and the two heating transitions was unambiguous after plotting the temperature dependences of the cell dimensions (Figures 2A and S7).

References

- ¹ Nonius. *COLLECT*; Nonius BV, Delft: The Netherlands, 1999.
- ² Schreurs, A. M. M. *PEAKREF*; University of Utrecht: The Netherlands, 2005.
- ³ Duisenberg, A. J. M.; Kroon-Batenburg, L. M. J.; Schreurs, A. M. M. *J. Appl. Cryst.* **2003**, *36*, 220.
- ⁴ Beurskens, P. T.; Beurskens, G.; de Gelder, R.; Garcia-Granda, S.; Gould, R. O.; Israel, R.; Smits, J. M. M. *The DIRDIF99 Program System, Technical Report of the Crystallography Laboratory*; University of Nijmegen: The Netherlands, 1999.
- ⁵ Sheldrick, G. M. *SHELXS86*; University of Göttingen: Germany, 1986.
- ⁶ Sheldrick, G. M. *Acta Cryst.* **2008**, *A64*, 112.
- ⁷ Sheldrick, G. M. *SADABS*; University of Göttingen: Germany, 1999–2003.
- ⁸ Sheldrick, G. M. *TWINABS*; University of Göttingen: Germany, 2003.
- ⁹ Duisenberg, A. J. M. *J. Appl. Cryst.* **1992**, *25*, 92.
- ¹⁰ Duisenberg, A. J. M.; Hooft, R. W. W. ; Schreurs, A. M. M.; Kroon, J. *J. Appl. Cryst.* **2000**, *33*, 893.

Figure S1. 1-D supramolecular chain for complex **1** (phase **I**) along which hydrogen bonding (green dotted lines) and π - π stacking interactions (red dotted lines) are found. H-bonded hydrogen atoms and ring centroids refer to Table S1 and S3, respectively. Symmetry code: $i = x, -y + 1, z + \frac{1}{2}$.

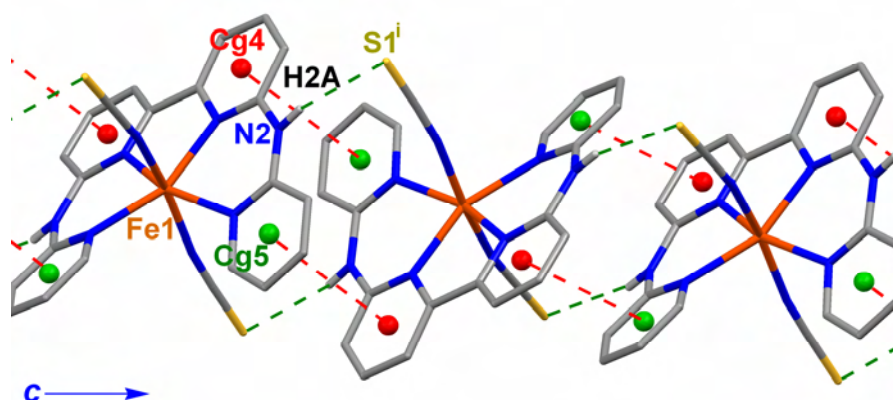


Figure S2. A) Asymmetric unit of Phase **II** of **1**. The Fe2(II) HS complex has twofold symmetry. B) Asymmetric unit of Phase **III** of **1**.

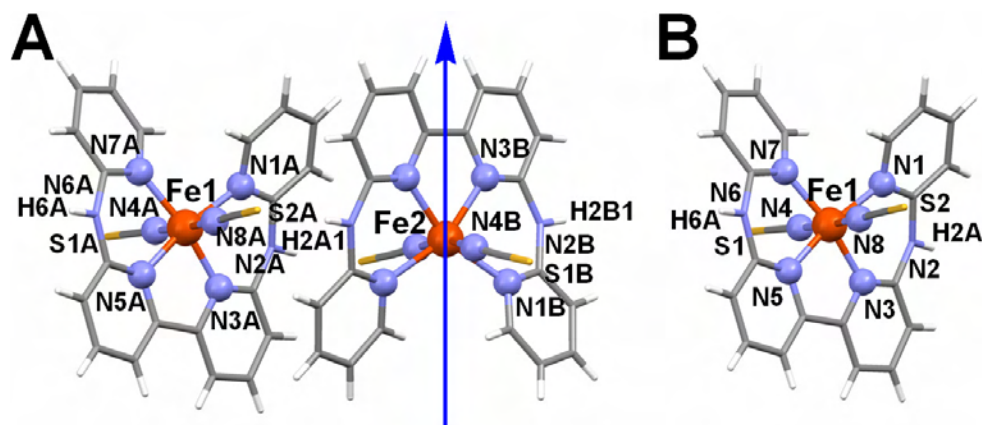


Figure S3. 1-D supramolecular chain for a) phase **II** and b) phase **III** of complex **1**, along which hydrogen bonding (green dotted lines) and π - π stacking interactions (red dotted lines) are found. H-bonded hydrogen atoms and ring centroids refer to Table S2 and S3, respectively. Symmetry codes: (ii) $-x + 1, -y + 1, -z$; (iii) $-x + 1, -y + 1, -z + 1$.

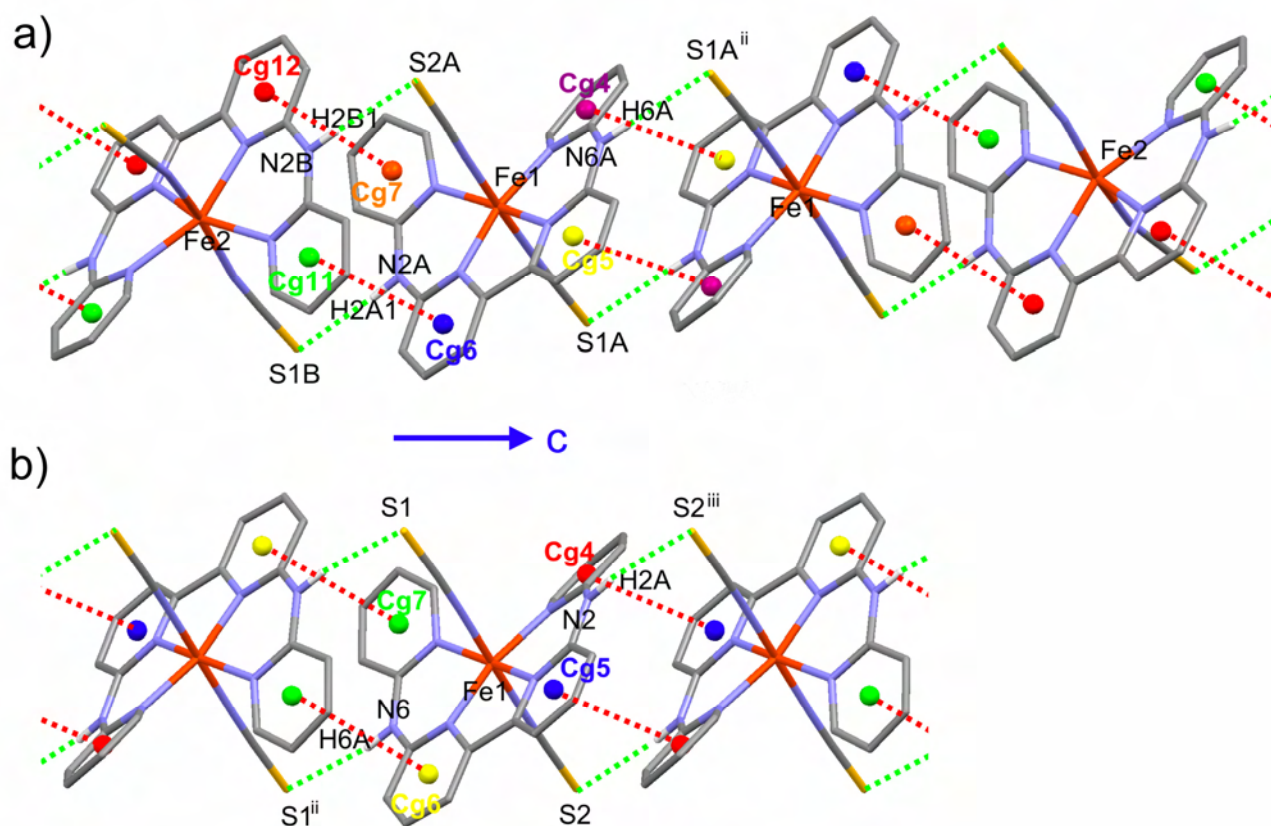


Table S1. Selected bond distances (Å) and angles (°) for the three phases of complex **1** (see Figures 1 and S2 for atom numbering). High-Spin distances are in **red** and Low-Spin distances in **blue**.

Phase I (HS)		Phase II (intermediate)			Phase III (LS)		
<i>Bond distances</i>							
Fe1-N1	2.1457(15)	Fe2-N1B	2.135(2)	Fe1-N1A	1.980(2)	Fe1-N1	1.980(2)
Fe1-N3	2.1350(15)	Fe2-N3B	2.131(2)	Fe1-N3A	1.942(2)	Fe1-N3	1.942(2)
Fe1-N4	2.1481(18)	Fe2-N4B	2.149(3)	Fe1-N4A	1.932(2)	Fe1-N4	1.933(2)
				Fe1-N5A	1.942(2)	Fe1-N5	1.943(2)
				Fe1-N7A	1.983(2)	Fe1-N7	1.987(2)
				Fe1-N8A	1.936(2)	Fe1-N8	1.942(2)
<i>Angles</i>							
N1-Fe1-N3	85.74(6)	N1B-Fe2-N3B	85.76(8)	N1A-Fe1-N3A	91.41(9)	N1-Fe1-N3	91.41(9)
N3-Fe1-N3a	77.34(8)	N3B-Fe2-N3Ba	77.47(12)	N3A-Fe1-N5A	82.46(9)	N3-Fe1-N5	82.67(9)
N1a-Fe1-N3a	85.74(6)	N3Ba-Fe2-N1Ba	85.76(8)	N5A-Fe1-N7A	92.13(9)	N5-Fe1-N7	92.22(9)
N1a-Fe1-N1	113.78(9)	N1Ba-Fe2-N1B	113.44(12)	N7A-Fe1-N1A	95.83(9)	N7-Fe1-N1	95.58(9)
N4a-Fe1-N4	167.67(10)	N4Ba-Fe2-N4B	167.70(13)	N4A-Fe1-N8A	177.30(9)	N4-Fe1-N8	177.34(10)

Symmetry operation: a = 1-x, y, 1/2-z

Table S2. N–H \cdots S interactions (\AA , $^\circ$) found in the three phases of complex **1** (see Figures S1 & S3).

N–H \cdots S	N–H	H \cdots S	N \cdots S	N–H \cdots S
Phase I				
N2–H2A \cdots S1 ⁱ	0.84(2)	2.58(2)	3.424(2)	178(2)
Phase II				
N2A–H2A1 \cdots S1B	0.86(2)	2.51(2)	3.371(2)	175(3)
N6A–H6A \cdots S1A ⁱⁱ	0.86(2)	2.50(2)	3.356(2)	173(3)
N2B–H2B1 \cdots S2A	0.87(2)	2.53(2)	3.390(2)	176(3)
Phase III				
N2–H2A \cdots S2 ⁱⁱⁱ	0.86(2)	2.53(2)	3.367(2)	165(3)
N6–H6A \cdots S1 ⁱⁱ	0.87(2)	2.48(2)	3.342(2)	170(3)

Symmetry codes: (i) $x, -y + 1, z + 1/2$; (ii) $-x + 1, -y + 1, -z$; (iii) $-x + 1, -y + 1, -z + 1$.

Table S3. π – π interactions found in the three phases of complex **1** (see Figures S1 & S3)

Phase I	
Cg4 \cdots Cg5	3.881(1) \AA
Phase II	
Cg4 \cdots Cg5	4.021(2) \AA
Cg6 \cdots Cg11	3.820(2) \AA
Cg7 \cdots Cg12	3.908(1) \AA
Phase III	
Cg4 \cdots Cg5	3.844(1) \AA
Cg6 \cdots Cg7	4.055(1) \AA

Figure S4. Projections of the three phases of **1** down the **b** direction. For phase **III**, the *a* and *c* axes are not in the plane of the drawing. The drawing shows that the packing is very similar in the three phases.

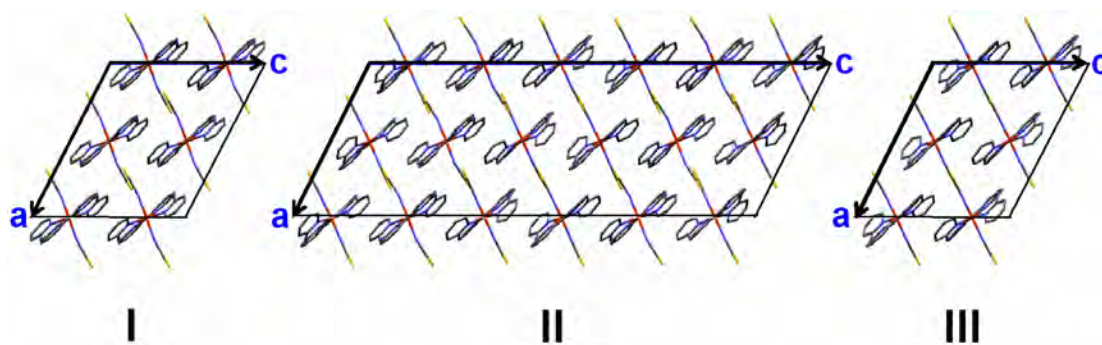


Figure S5. Crystal packing of the intermediate phase **II** of **1** looking down the **b** direction. The drawing illustrates the 1-D supramolecular chains built of the repetitive [HS...LS...LS] motif along the *c* direction. The HS Fe(II) centres are shown in red (space filling mode) and the LS Fe(II) centres are shown in blue (space filling mode). The H bonding and π - π stacking interactions are not shown for the sake of clarity.

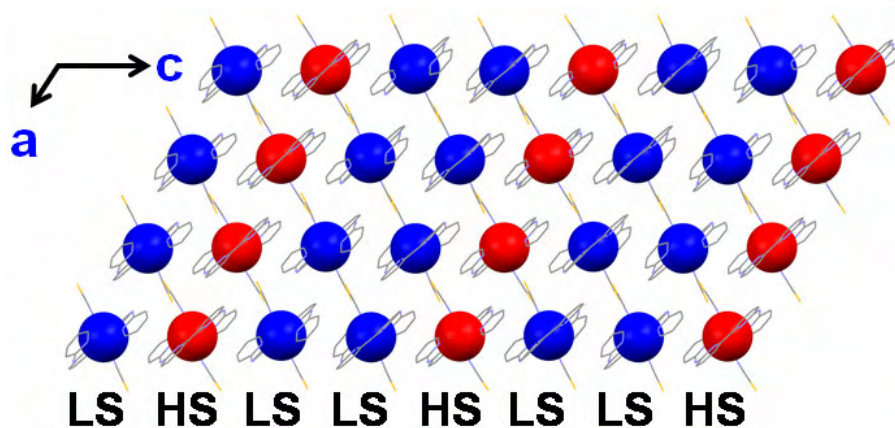


Figure S6. Parts of the reciprocal lattice slices $0kl$ digitally reconstructed from the measured frames given for phase **I** (295 K), for phase **II** (190 K) and for phase **III** (110 K). At 190 K, extra Bragg reflections are found along the c^* direction. At 110 K, the non-overlap reflections are obvious and the crystal is non-merohedrally twinned.

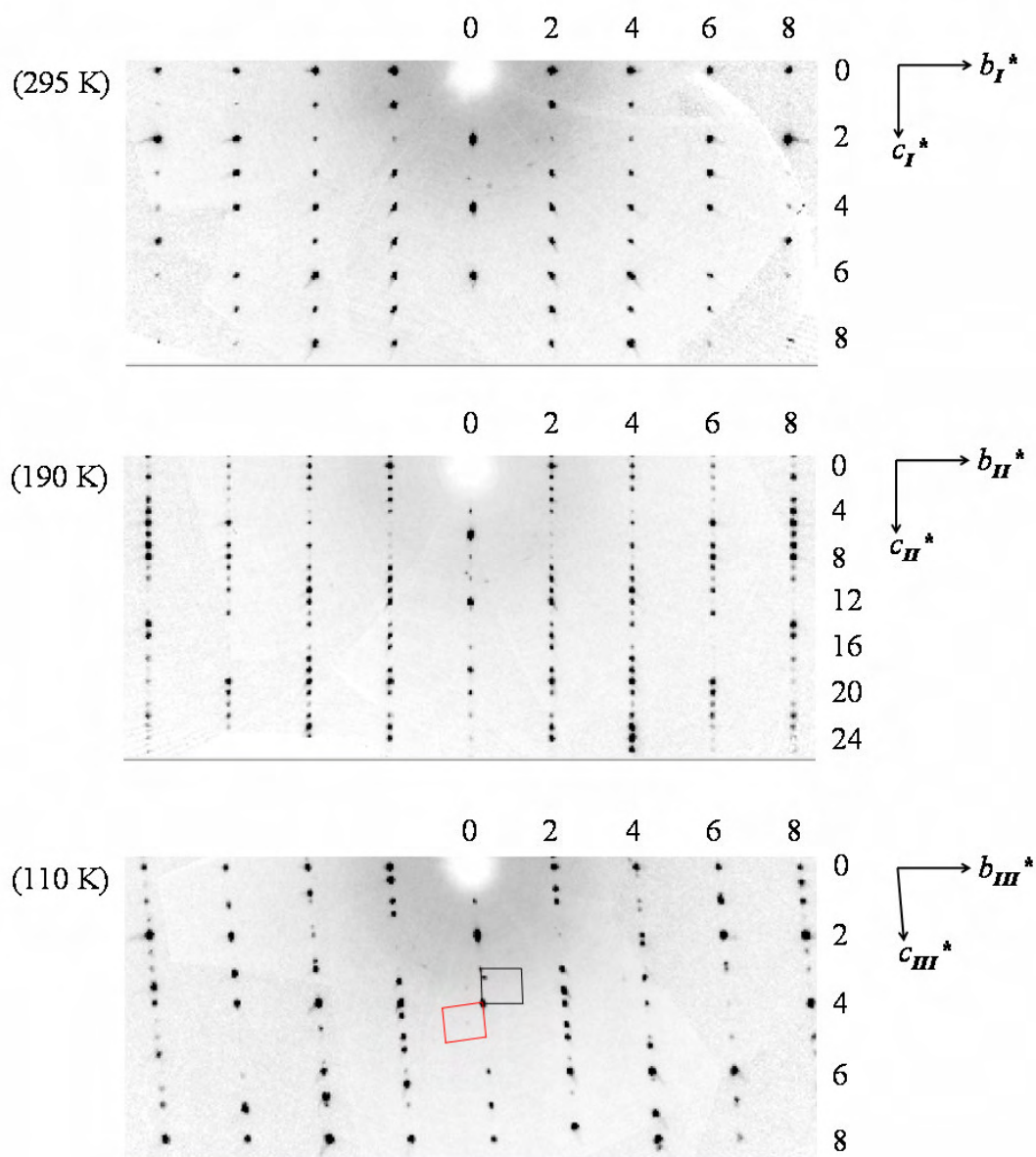
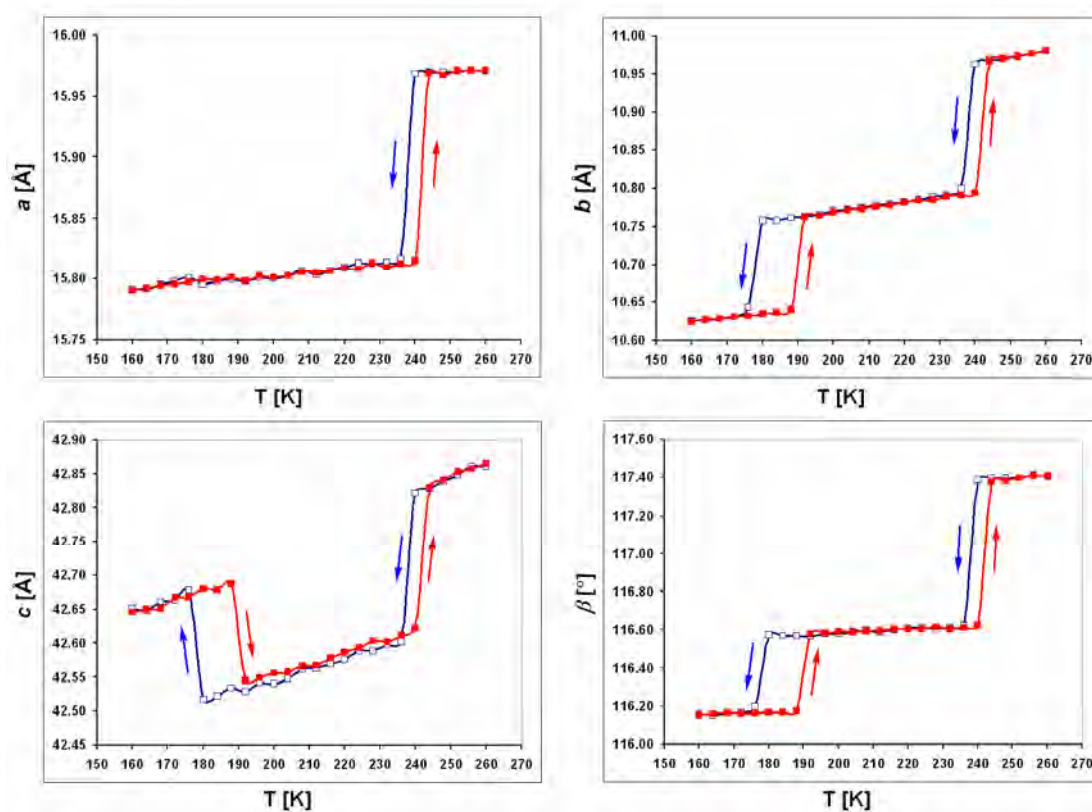


Figure S7. Plots of the cell dimensions a (Å), b (Å), c (Å) and β (°) for **1** determined from 260 to 160 K at -4 K intervals and from 160 to 260 K at 4 K intervals. Discontinuities are found near 178 and 238 K for the cooling transitions (blue curves), and near 190 and 242 K for the heating transitions (red curves). The hysteresis widths for the lower- and higher-temperature transitions are about 12 and 4 K. Errors bars are not reported since they are not significant compared to the axis scales. The c axes for phases **I** and **III** were multiplied by a factor of 3 to minimize Δc at the two transitions.



Differential Scanning Calorimetry (DSC)

DSC measurements were carried out on a Netsch DSC 204 instrument under helium purging gas ($20 \text{ cm}^3 \text{ min}^{-1}$) at a scan rate of 10 K min^{-1} in both heating and cooling modes. Temperature and enthalpy (ΔH) were calibrated using the melting transition of standard materials (Hg, In, Sn). The uncertainty in the transition enthalpy (ΔH) and entropy (ΔS) is estimated of *ca.* 10 % due to the subtraction of the unknown baseline and uncertainties in the residual (*i.e.* non-transformed) fractions.

Note: the calculated enthalpy/entropy changes are given per metal ion involved in each step of the transition.

Figure S8. DSC analysis for **1**. The first and second transitions are observed at 230 K and 169 K in the cooling mode, and at 240 K and 193 K in the heating mode.

